Effective Theranostic Cyanine for Imaging of Amyloid Species in vivo and Cognitive Improvements in Mouse Model

Yinhui Li,[1,4] Chen Chen,[1,2] Di Xu,[1,3] Chung-Yan Poon,[1] See-Lok Ho,[1] Rui Zheng,[2] Qiong Liu,[2] Guoli Song,[2*] Hung-Wing Li,[1*] and Man Shing Wong[1,3 *]

[1]Department of Chemistry, Hong Kong Baptist University, Kowloon Tong, Hong Kong SAR (China).

[2]Shenzhen Key Laboratory of Marine Biotechnology and Ecology, College of Life Sciences, Shenzhen University, Shenzhen, (China)

[3]The Institute of Molecular Functional Materials, Hong Kong Baptist University, Kowloon Tong, Hong Kong SAR (China)

[4]Key Laboratory for Green Organic Synthesis and Application of Hunan Province, Key Laboratory of Environmentally Friendly Chemistry and Application of Ministry of Education, College of Chemistry, Xiangtan University, Xiangtan, 411105 (China)

‡ Yinhui Li, Chen Chen and Di Xu contributed equally to this work

Corresponding author E-mail: mswong@hkbu.edu.hk; hwli@hkbu.edu.hk; lilys@szu.edu.cn

Supporting Information

Experimental Section

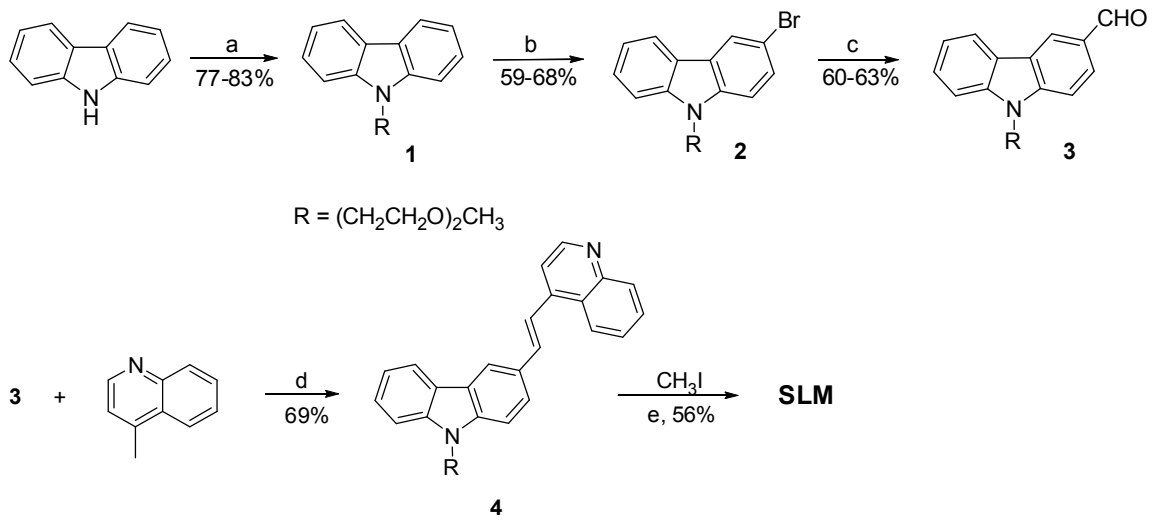

Reagents and Conditions: a, $(CH_2CH_2O)_2CH_3$, NaH, DMF, 80 °C; b, NBS, DCM, 0 °C to r.t.; c, *n*-BuLi, DMF, THF, −78 °C to r.t.; d, TMSCl, DMF, 100 °C, sealed tube; e, CH_3CN, r.t.

Scheme S1. Synthesis of SLM.

Synthetic Procedure of SLM. Compound **1**, **2** and **3** were prepared by the literature protocols.[1] A solution mixture of **4** (0.6 mmol) and CH_3I (0.6 mmol) in ethanol (40 mL) was stirred at room temperature. After the reaction completed, the organic solvent was removed. The residue was purified by recrystallization from methanol to afford **SLM** as a red solid in 56% yield. ^{1}H NMR (400 MHz, DMSO-d_6) δ 9.28 (d, J = 6.4 Hz, 1H), 9.14 (d, J = 8.4 Hz, 1H), 8.86 (s, 1H), 8.51 (d, J = 6.4 Hz, 1H), 8.42 (m, 3H), 8.28 (m, 2H), 8.13 (d, J = 8.8 Hz, 1H), 8.08 (t, J = 7.2 Hz, 1H), 7.80 (d, J = 8.8 Hz, 1H), 7.71 (d, J = 8.0 Hz, 1H), 7.53 (t, J = 8.0 Hz, 1H), 7.32 (t, J = 7.2 Hz, 1H), 4.64 (t, J = 5.2 Hz, 2H), 4.52 (s, 3H), 3.84 (t, J = 5.2 Hz, 2H), 3.48 (m, 2H), 3.33 (m, 2H), 3.11 (s, 3H). ^{13}C NMR (100 MHz, DMSO-d_6) δ 153.0, 147.0, 144.9, 142.1, 140.9, 138.8, 134.9, 129.0, 127.3, 126.7, 126.4, 126.1, 122.8, 122.2, 121.7, 120.4, 119.9, 119.3, 116.2, 115.1, 110.5, 110.4, 71.3, 69.8, 68.9, 58.1, 44.2, 42.9. HRMS (MALDI-TOF) *m/z* Calcd for $C_{29}H_{29}N_2O_2$ 437.2223 Found 437.2207 [M^+].

Table S1. Physical properties of **SLM** and its dissociation constants (K_d) with monomeric and fibrillar $A\beta_{(1\text{-}40)}$ and $A\beta_{(1\text{-}42)}$.

Dye	λ^{abs}_{max}/ λ^{abs}_{max} (nm)	K_d fibril(Aβ40) μM	K_d mon(Aβ40) μM	K_d fibril(Aβ42) μM	K_d mon(Aβ42) μM	Log P
SLM	455/676	13.1	96.6	11.4	40.2	2.59

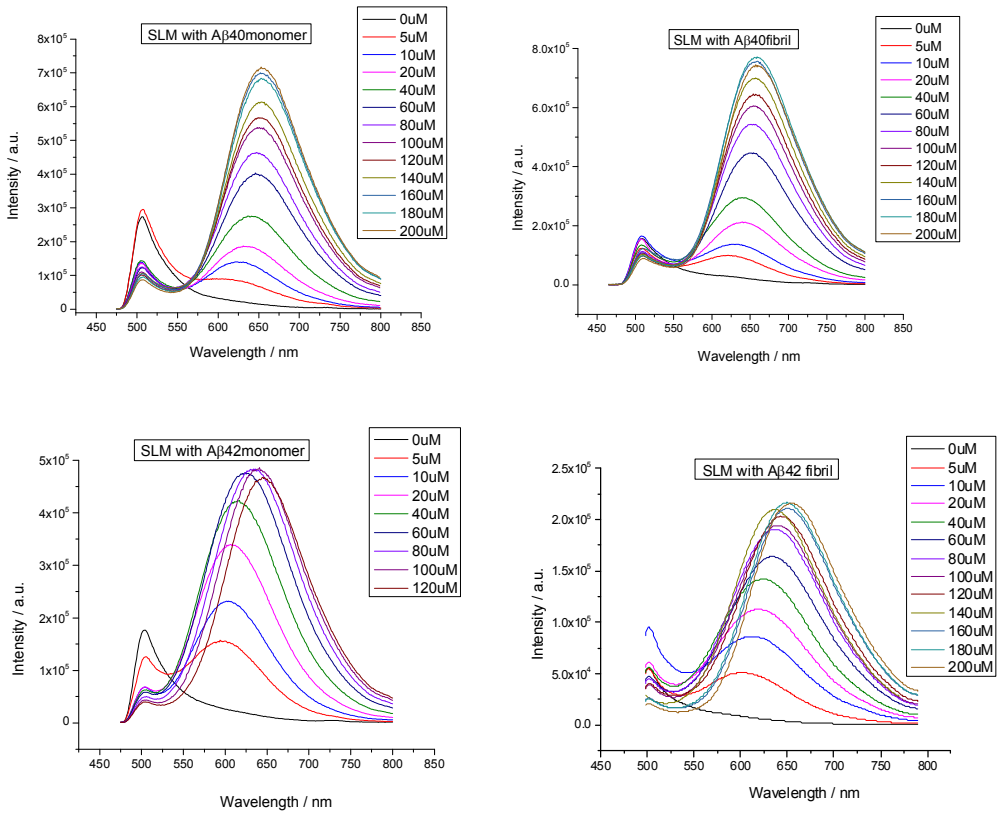

Figure S1 Fluorescence titrations of **SLM** with $A\beta_{(1\text{–}40)}$ monomer and fibrils as well as $A\beta_{(1\text{–}42)}$ monomer and fibrils.

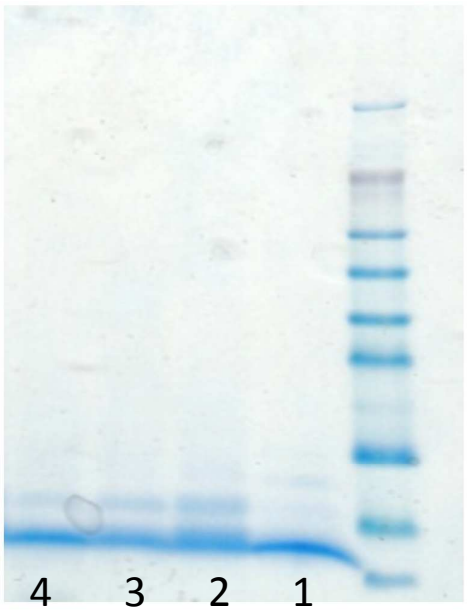

Figure S2 The oligomerization of $A\beta_{(1-42)}$ was inhibited by **SLM**, as revealed by SDS-PAGE. The outside lane represents the molecular weight markers; Lane 1, HFIP treated 100 μM monomeric $A\beta_{(1-42)}$; Lane 2, 100 μM oligomeric $A\beta_{(1-42)}$ by incubating monomer at 4°C for 24 h; (c) Lane 3-4, in the addition of **SLM**; at 1:1 and 5:1 molar ratio of cyanine-to-peptide, respectively. The intensity of the band of the dimeric was weaker when higher concentration of **SLM** was applied, suggesting the inhibitory effect on $A\beta_{(1-42)}$ oligomerization.

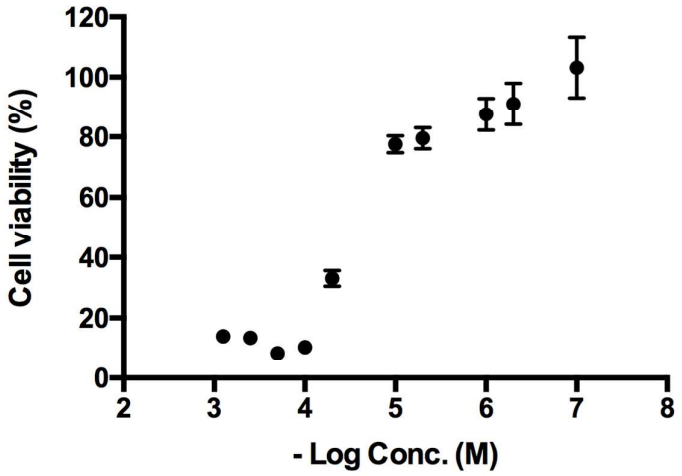

Figure S3. LC50 of SLM as assessed by the MTT assay.

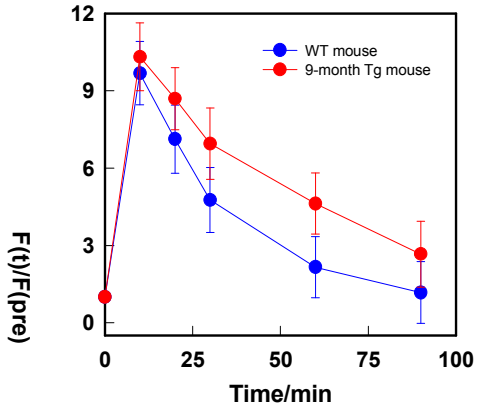

Figure S4. The relative fluorescence signal [F(t)/F(pre)] in the brain regions of Tg (9-month old) and WT mice after IV injection of **SLM**. The [F(t)/F(pre)] of Tg mouse was significantly higher than that of WT mouse ($p < 0.05$).

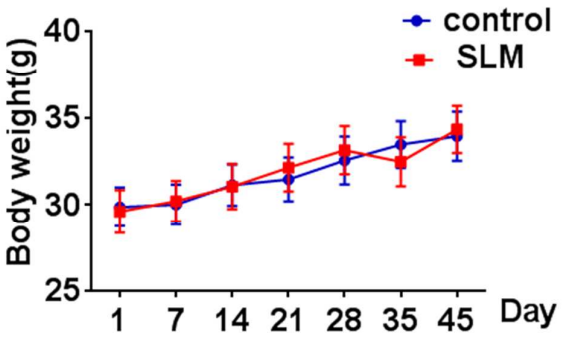

Figure S5. The body weights of the control and **SLM** treated mice after IP injection were monitored once a week.

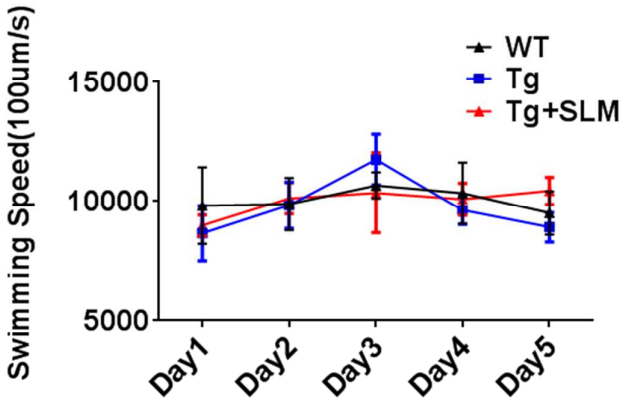

Figure S6. In the Morris Water Maze assessment, the swimming speed of the mice between the three groups was compared and it suggested that there was no significantly difference in the swimming ability.

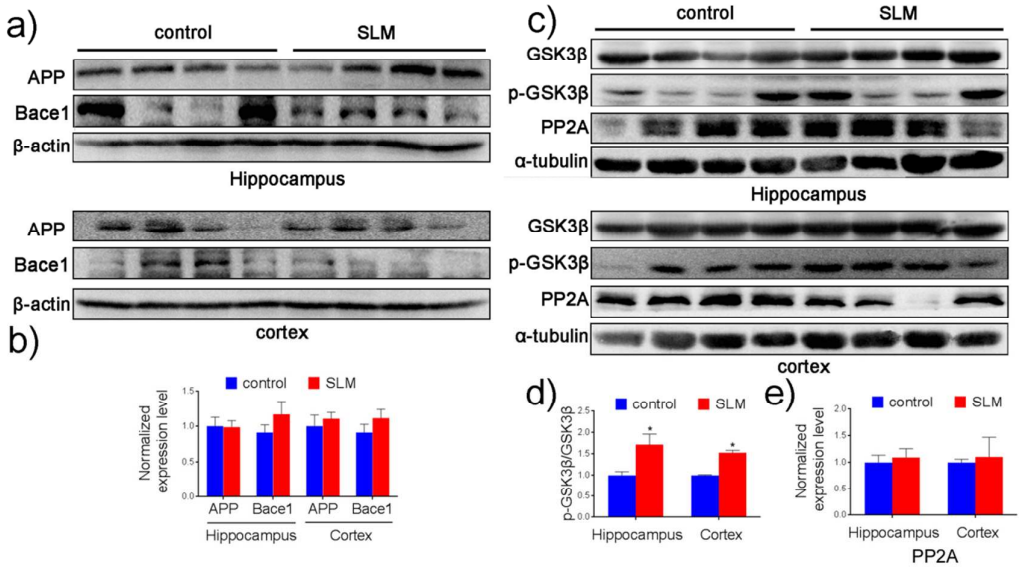

Figure S7. Upon **SLM** treatment, the level of inactive phosphorylated glycogen synthase kinase-3β (p-GSK3β) (c-d) was significantly higher in the **SLM**-treated Tg mice. Nonetheless, the level of APP (a, b) and Bace 1 (a-b), PP2A (c, e) were similar as compared to the un-treated Tg mice indicating the production of Aβ was not disrupted by the **SLM** treatment.

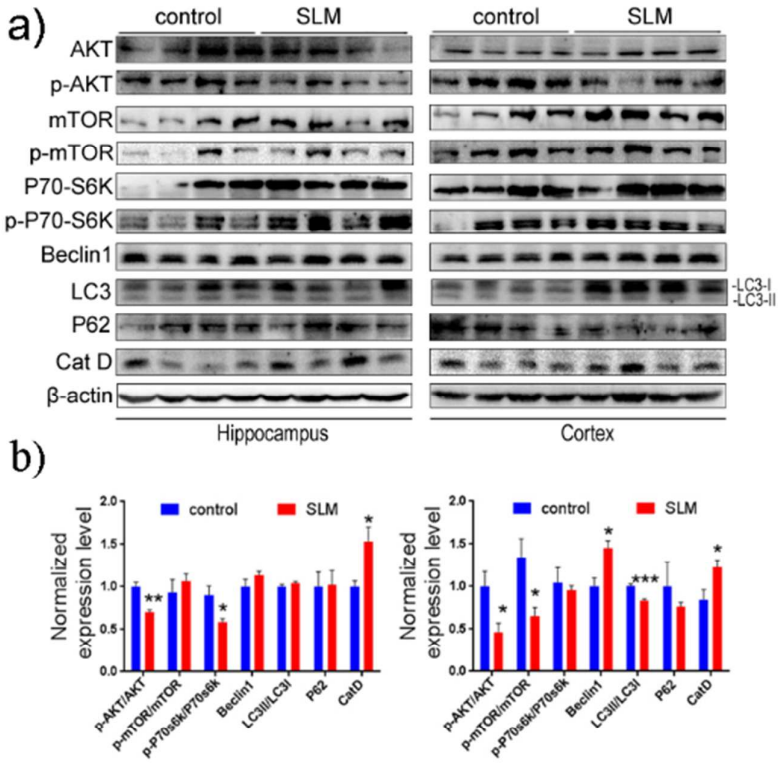

Figure S8. Upon **SLM** treatment, there was a significantly reduced level of mammalian target of rapamycin (mTOR)(a-b), a key gatekeeper of autophagy, which was down-regulated by the substantial decrease in an upstream effector, Akt(a-b); and an increase in the mammalian orthologue of yeast Atg6 (Beclin 1) level(a-b), a proautophagic protein. In addition, there was a markedly reduced level of microtubule-associated protein light chain 3-II (LC3-II) (a-b) and the LC3-associated protein p62 (sequestosome 1) (a-b), a marker of autophagic flux. The level of the lysosomal protease Cathepsin D (CatD) (a-b) that mediates the degradation in autophagolysosomes was found to be significantly increased.

a)

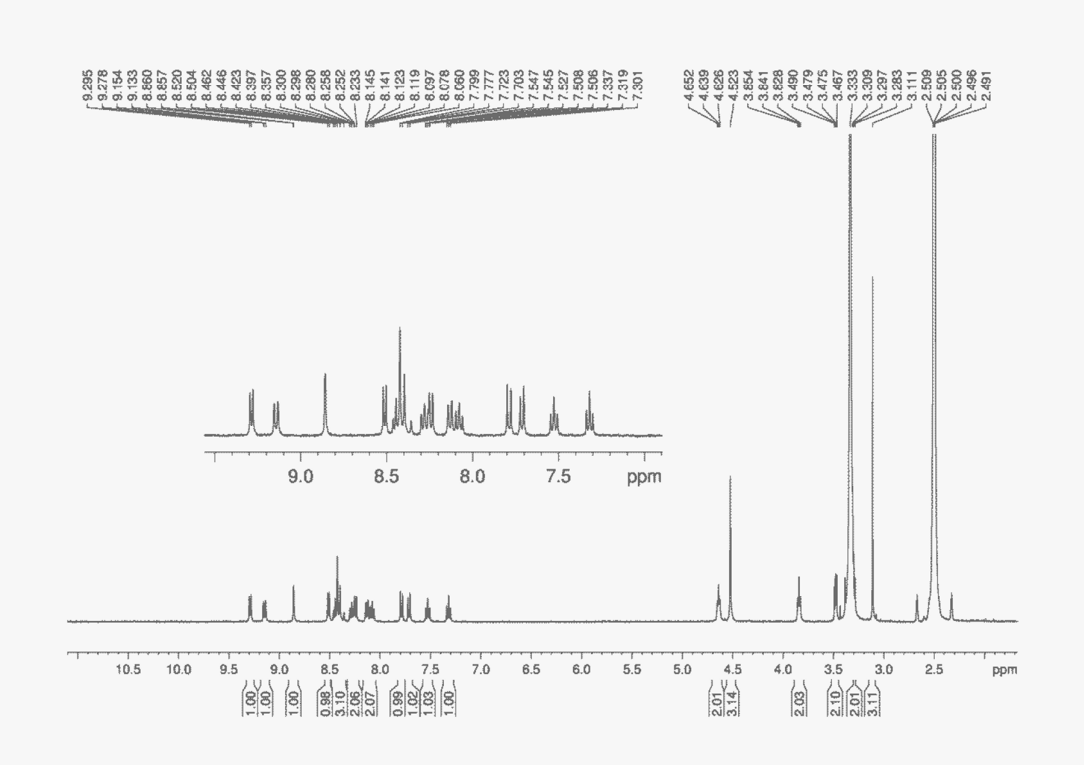

b)

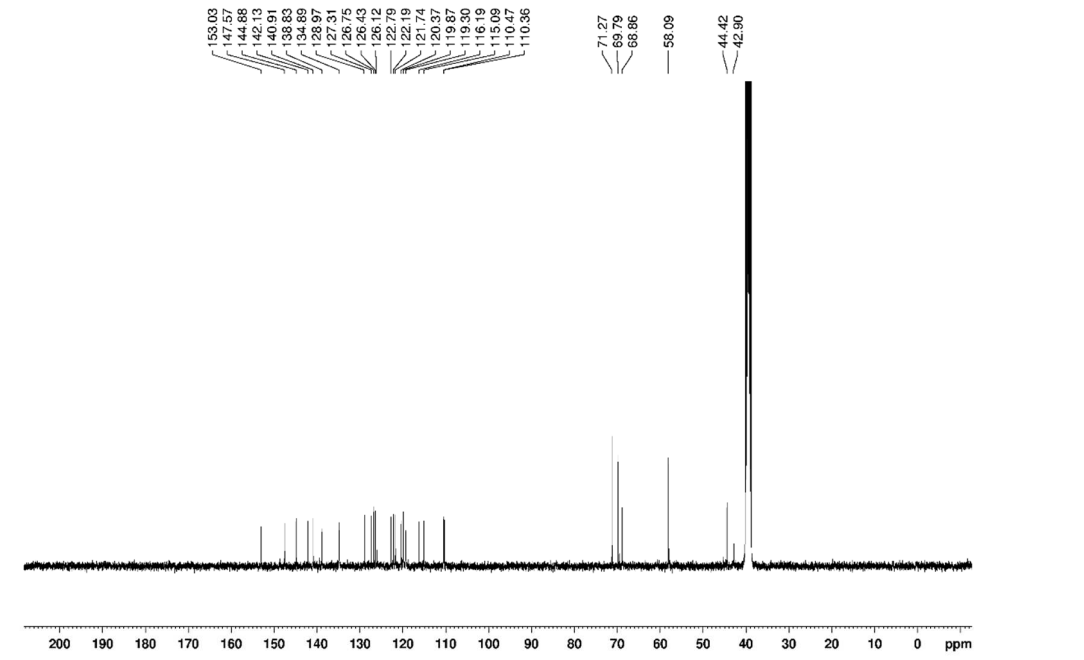

Figure S9. ^{1}H NMR (400 MHz, DMSO-d_6) and ^{13}C NMR (100 MHz, DMSO-d_6) spectra of **SLM**.

Reference:

1. Yang, W. G.; Wong, Y.; Ng, O. T. W.; Bai, L. P.; Kwong, D. W. J.; Ke, Y.; Jiang, Z. H.; Li, H. W.; Yung, K. K. L.; Wong, M. S. *Angew. Chem. Int. Ed.* **2012**, *51*, 1804.